OPEN ACCESS Freely available online

PLOS ONE

# Dopamine $D_1$, $D_2$, $D_3$ Receptors, Vesicular Monoamine Transporter Type-2 (VMAT2) and Dopamine Transporter (DAT) Densities in Aged Human Brain

**Jianjun Sun[1¤], Jinbin Xu[1], Nigel J. Cairns[2,3], Joel S. Perlmutter[1,2,4,5,6], Robert H. Mach[1,7,8]***

**1** Department of Radiology, Washington University School of Medicine, St. Louis, Missouri, United States of America, **2** Department of Neurology, Washington University School of Medicine, St. Louis, Missouri, United States of America, **3** Department of Pathology and Immunology, Washington University School of Medicine, St. Louis, Missouri, United States of America, **4** Department of Neurobiology, Washington University School of Medicine, St. Louis, Missouri, United States of America, **5** Department of Occupational Therapy, Washington University School of Medicine, St. Louis, Missouri, United States of America, **6** Department of Physical Therapy, Washington University School of Medicine, St. Louis, Missouri, United States of America, **7** Department of Cell Biology amd Physiology, Washington University School of Medicine, St. Louis, Missouri, United States of America, **8** Biochemistry and Molecular Biophysics, Washington University School of Medicine, St. Louis, Missouri, United States of America

## Abstract

The dopamine $D_1$, $D_2$, $D_3$ receptors, vesicular monoamine transporter type-2 (VMAT2), and dopamine transporter (DAT) densities were measured in 11 aged human brains (aged 77–107.8, mean: 91 years) by quantitative autoradiography. The density of $D_1$ receptors, VMAT2, and DAT was measured using [$^3$H]SCH23390, [$^3$H]dihydrotetrabenazine, and [$^3$H]WIN35428, respectively. The density of $D_2$ and $D_3$ receptors was calculated using the $D_3$-preferring radioligand, [$^3$H]**WC-10** and the $D_2$-preferring radioligand [$^3$H]raclopride using a mathematical model developed previously by our group. Dopamine $D_1$, $D_2$, and $D_3$ receptors are extensively distributed throughout striatum; the highest density of $D_3$ receptors occurred in the nucleus accumbens (NAc). The density of the DAT is 10–20-fold lower than that of VMAT2 in striatal regions. Dopamine $D_3$ receptor density exceeded $D_2$ receptor densities in extrastriatal regions, and thalamus contained a high level of $D_3$ receptors with negligible $D_2$ receptors. The density of dopamine $D_1$ linearly correlated with $D_3$ receptor density in the thalamus. The density of the DAT was negligible in the extrastriatal regions whereas the VMAT2 was expressed in moderate density. $D_3$ receptor and VMAT2 densities were in similar level between the aged human and aged rhesus brain samples, whereas aged human brain samples had lower range of densities of $D_1$ and $D_2$ receptors and DAT compared with the aged rhesus monkey brain. The differential density of $D_3$ and $D_2$ receptors in human brain will be useful in the interpretation of PET imaging studies in human subjects with existing radiotracers, and assist in the validation of newer PET radiotracers having a higher selectivity for dopamine $D_2$ or $D_3$ receptors.

**Citation:** Sun J, Xu J, Cairns NJ, Perlmutter JS, Mach RH (2012) Dopamine $D_1$, $D_2$, $D_3$ Receptors, Vesicular Monoamine Transporter Type-2 (VMAT2) and Dopamine Transporter (DAT) Densities in Aged Human Brain. PLoS ONE 7(11): e49483. doi:10.1371/journal.pone.0049483

**Editor:** Bernard Le Foll, Centre for Addiction and Mental Health, Canada

**Received** August 3, 2012; **Accepted** October 11, 2012; **Published** November 21, 2012



**Funding:** This study was supported by NIH grants MH081281, DA29840, NS075321 and P50 AG05681, the American Parkinson Disease Association (APDA), the Greater St. Louis Chapter of the APDA, the Barnes-Jewish Hospital Foundation (Elliot Stein Family Fund and Parkinson Disease Research Fund) and the Charles and Joanne Knight Alzheimer's Research Initiative of the Washington University Alzheimer's Disease Research Center.The funders had no role in study design, data collection and analysis, decision to publish, or preparation of the manuscript.

**Competing Interests:** The authors have declared that no competing interests exist.

* E-mail: rhmach@mir.wustl.edu

¤ Current address: Neurosurgery Department, The Second Affiliated Hospital of Medical College, Xi'an Jiaotong University, Xi'an, Shaanxi, 710004, PR China

## Introduction

The dopaminergic system is involved in neurological disorders such as Parkinson disease, drug addiction and schizophrenia [1–4]. Dopamine receptors have been classified into two subtypes: $D_1$-like and $D_2$-like receptors. Stimulation of $D_1$-like ($D_1$ and $D_5$) receptors activates adenylate cyclase and increases cAMP (cyclic adenosine monophosphate) production. Stimulation of $D_2$-like ($D_2$, $D_3$ and $D_4$) receptors inhibits adenylate cyclase activity, increases arachadonic acid release and phosphatidylinositol hydrolysis [5,6]. The dopamine transporter (DAT) is a presynaptic membrane protein which is responsible for the reuptake of dopamine into dopaminergic nerve terminals. The vesicular monoamine transporter type-2 (VMAT2) is a vesicular membrane protein that transport monoamines from the cytosol into synaptic vesicles [7]. Both have been used as dopamine presynaptic markers for nigrostriatal neuronal integrity.

Since radioligands for PET imaging dopamine $D_2$-like receptors, such as the antagonists [$^{11}$C]raclopride [8], [$^{18}$F]fallypride [9] and the full agonist [$^{11}$C](+)-PHNO [10], bind to both the dopamine $D_2$ and $D_3$ receptors, PET studies can only measure the composite density of these receptors, the dopamine $D_2/D_3$ receptor binding potential. Quantitative autoradiography measuring dopamine $D_2$ and $D_3$ receptor densities have yielded equivocal receptor density values and distribution patterns in human and monkey brain [11–18]. This can be attributed to the low $D_2/D_3$ selectivity of all radioligands used in these studies. Some studies have attempted to quantify dopamine $D_3$ receptors using "selective" radiolabeled dopamine $D_3$ agonists (7-OH-DPAT, PIPAT and PD128947), but these ligands also bind to the high affinity agonist binding state of the $D_2$ receptor and require first

decoupling the $D_2$ receptor from G proteins to image the $D_3$ receptor. Studies using radiolabeled selective dopamine $D_3$ versus $D_2$ receptor antagonists are not well documented [5,18,19].

**WC-10**, a weak partial agonist/antagonist at the $D_3$ receptor, binds with a 66-fold higher affinity to human HEK $D_3$ than HEK $D_{2L}$ receptors, with a dissociation constant ($K_d$) of 1.2 nM at HEK $D_3$ receptors [19,20]. By using [$^3$H]**WC-10** and a $D_2/D_3$ ligand [$^3$H]raclopride, we have developed a quantitative autoradiography assay for measuring the absolute densities of dopamine $D_2$ and $D_3$ receptors in the striatal regions of rat and rhesus monkey brain [18]. In this study, the absolute densities of dopamine $D_2$ and $D_3$ receptors were determined by using the same autoradiography assay in the striatal and extrastriatal regions of an aged monkey (25 years old) and aged human brains (average age = 91, range = 77–107.8 years old). The dopamine $D_1$ receptor, DAT, and VMAT2 densities were also measured by quantitative autoradiography. The results of this study provide a unique measurement of the density of $D_1$, $D_2$ and $D_3$ receptors, and DAT and VMAT2 levels, in the same human brain samples.

## Materials and Methods

### Ethics Statement

After death, the written consent of the next of kin was obtained for brain removal, following local Ethical Committee procedures (Human Studies Committee, Washington University School of Medicine). Postmortem receptor autoradiography study has been approved by the Alzheimer's disease Research Center (ADRC) Committee; the approval letter is submitted as a supplement.

The monkey used in this study belongs to our group and was euthanized using pentobarbital 100 mg/kg i.v. due to age-related health decline. This method is consistent with the recommendations of the Panel on Euthanasia of the American Veterinary Medical Association. These studies have been approved by the IACUC at Washington University (approval #20110161). Washington University is fully accredited by the American Association for the Accreditation of Laboratory Animal Care (AAALAC).

### Precursor synthesis and radiolabeling

[$^3$H]**WC-10** (Figure 1) was synthesized by American Radiolabeled Chemicals (St Louis, Missouri, USA) by alkylation of the desmethyl precursor with [$^3$H]methyl iodide. The specific activity of the radioligand was 80 Ci/mmol. The detailed synthesis scheme for [$^3$H]**WC-10** has been previously described [19].

### Drugs

Chemical reagents and the standard compounds were purchased from Sigma (St. Louis, MO) and Tocris (Ellisville, MO). [$^3$H]raclopride (76 Ci/mmol), [$^3$H]SCH23390 (85 Ci/mmol) and [$^3$H]WIN35428 (76 Ci/mmol) were purchased from Perkin Elmer Life Sciences (Boston, MA). [$^3$H]dihydrotetrabenazine ([$^3$H]DTBZ) (20 Ci/mmol) was purchased from American Radiolabeled Chemicals (St Louis, Missouri, USA).

### Tissue collection

Clinically and neuropathologically well-characterized human brain tissues were obtained from the Knight Alzheimer's Disease Research Center, Washington University School of Medicine. All cases were longitudinally assessed, healthy elderly individuals without neurological or psychiatric disease and included 4 males and 7 females, aged 77–107.8 (mean: 91) years. Table 1 shows the demographic case variables. Brains were removed at autopsy and the right hemibrain was coronally sliced and snap-frozen by contact with Teflon-coated aluminum plates cooled in liquid nitrogen vapor, subsequently stored in zip-lock airtight plastic bags and stored at −80°C until used. Microscopy was performed using established rating scales. Alzheimer's disease pathological changes were assessed using Braak staging [21,22]. For autoradiography studies, frozen coronal sections (20 μm) were cut with a Microm cryotome and mounted on Superfrost Plus glass slides (Fisher Scientific, Pittsburgh, PA) from following brain regions: precommissural striatal regions containing the caudate, putamen and nucleus accumbens (NAc); globus pallidus (GP) containing the internal and external part (GPi and GPe); thalamus containing postcommissural striatal regions; and middle brain containing substantia nigra (SN) and red nucleus (RN). For the determination of total binding, data from 2–4 sections were averaged and nonspecific binding was defined by average of 1–2 adjacent sections for all the radioligands. Another set of adjacent sections used for cresyl violet staining to identify related anatomical structures.

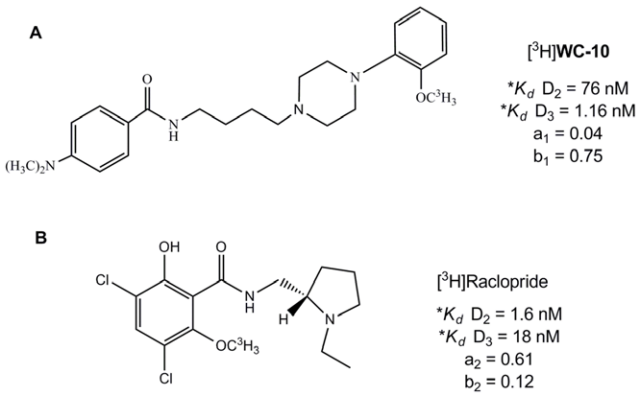


**Figure 1. Chemical structures of [$^3$H]WC-10 and [$^3$H]raclopride.** $K_d$ values were obtained through saturation binding of [$^3$H]**WC-10** and [$^3$H]raclopride to cloned human $D_3$ and $D_{2L}$ receptors expressed in HEK cells. $a_1$, and $b_1$ represent the fractional receptor occupancy to dopamine $D_2$ and $D_3$ receptors in human brain at a ligand concentration of 3.54 nM for [$^3$H]**WC-10**. $a_2$ and $b_2$ represent the same parameters at a ligand concentration of 2.50 nM [$^3$H]raclopride. The receptor occupancy fractions were calculated from the saturation binding isotherm using the $K_d$ values. *Data were taken from Xu et al. (2009).
doi:10.1371/journal.pone.0049483.g001

### Quantitative autoradiography protocol

Sections for dopamine $D_1$, $D_2$, and $D_3$ receptor binding were pre incubated for 20 min at room temperature in buffer (50 mM Tris buffer, pH 7.4, containing 120 mM NaCl, 5 mM KCl) to remove endogenous dopamine. After incubation with the respective radiotracer, slides were then rinsed five times at 1 min intervals with ice-cold buffer. Slides were incubated in an open staining jar, with the free radioligand concentration loss at less than 5% as previously described [18,19].

**Dopamine $D_1$ receptor binding.** $D_1$ receptors were labeled with [$^3$H]SCH23390 using the procedure described by Savasta [23] with minor modifications. Briefly, after preincubation to remove endogenous dopamine, sections were incubated for 60 min at room temperature in a similar buffer solution with the addition of 1.44 nM [$^3$H]SCH23390 and 30 nM ketanserin tartrate (Tocris Bioscience, Ellisville, Missouri, USA) to block 5-$HT_2$ receptors. Nonspecific binding was determined in the presence of 1 μM (+)-butaclamol as described previously [24,25].

**Dopamine $D_2$ receptor binding.** $D_2$ receptors were labeled with [$^3$H]raclopride using the previously described procedure for

**Table 1.** Demographic details of human brains.

| Autopsy number | Age(y) | Gender | Brain Weight(g) | PMI(h) | Braak NFT | Braak Amyloid | CDR |
|---|---|---|---|---|---|---|---|
| 105.460 | 77 | F | 1410 | 10 | 1 | A | 0 |
| 107.050 | 96 | M | 1165 | 12 | 1 | 0 | 0 |
| 100.060 | 91.6 | F | 1310 | 16 | 2 | 0 | 0 |
| 105.210 | 107.8 | F | 1080 | 5 | 2 | A | 0 |
| 101.200 | 92.1 | F | 1120 | 6 | 0 | 0 | 0 |
| 104.300 | 91.6 | F | 1220 | 16 | 2 | A | 0 |
| 11.027 | 79 | F | 1100 | 25 | 1 | A | 0 |
| 11.041 | 100 | F | 1450 | 21 | 2 | C | 0 |
| 10.740 | 90 | M | 1150 | 10 | 4 | A | 0 |
| 10.150 | 84 | M | 1010 | 5.5 | 1 | B | 0 |
| 9.255 | 91 | M | 1170 | 8.5 | 1 | A | 0 |

PMI: Post-mortem interval; CDR: Clinical dementia rating.
doi:10.1371/journal.pone.0049483.t001

rat and monkey tissue [18]. Brain sections were incubated for 60 min in buffer solution at room temperature with the addition of 2.50 nM [$^3$H]raclopride. Nonspecific binding was determined from the slides in the presence of 1 μM *S*-(–)-eticlopride [18].

**Dopamine $D_3$ receptor binding.** $D_3$ receptors were labeled with [$^3$H]**WC-10** using the previously described procedure for rat and monkey tissue [18]. Brain sections were incubated for 60 min in buffer solution at room temperature with the addition of 3.54 nM [$^3$H]**WC-10**, 10 nM WAY-100635 was added to solution to block 5-$HT_{1A}$ receptors. Nonspecific binding was determined in the presence of 1 μM *S*-(–)-eticlopride [18].

**DAT binding.** DAT were labeled with [$^3$H]WIN35428. Brain sections were incubated for 60 min in buffer solution at room temperature with the addition of 2.19 nM [$^3$H]WIN35428. Nonspecific binding was determined from the slides in the presence of 1 μM nomifensine.

**VMAT2 binding.** VMAT2 binding sites were labeled with [$^3$H]DTBZ. Brain sections were incubated for 60 min in buffer solution at room temperature with the addition of 4.53 nM [$^3$H]DTBZ. Nonspecific binding was determined from the slides in the presence of 1 μM *S*-(–)tetrabenazine.

**Quantification of total radioactivity.** Slides were air dried and made conductive by coating the free side with a copper foil tape. Slides were then placed into a gas chamber containing a mixture of argon and triethylamine (Sigma-Aldrich, USA) as part of a gaseous detector system, the Beta Imager 2000Z Digital Beta Imaging System (Biospace, France). After the gas was well mixed and a homogenous state was reached, further exposure for 20 h yielded high-quality images. A [$^3$H]Microscale (American Radiolabeled Chemicals, St Louis, Missouri, USA) was counted simultaneously as a reference for total radioactivity quantitative analysis. Quantitative analysis was performed with the program Beta-Vision Plus (BioSpace, France) for each anatomical region of interest.

**Cresyl violet staining.** A set of adjacent sections was fixed with 4% paraformaldehyde for 10 min, washed with PBS for 1 min, then dipped in 100% ethanol for 20 seconds to remove fat and fixation chemicals. Sections were then stained with 0.5% cresyl violet solution for 3 min, washed in running tap water 10 min, dehydrated by a series of alcohol baths, and made transparent by xylene (2×4 min) and scanned with an Epson scanner.

**Determination of absolute densities of $D_2$ and $D_3$ receptors.** Measurement of the absolute densities of dopamine $D_2$ and $D_3$ receptors using the $D_3$ selective radioligand [$^3$H]**WC-10** and the $D_2/D_3$ ligand, [$^3$H]raclopride was described previously [18]. Briefly, the receptor fractional occupancy of [$^3$H]**WC-10** and [$^3$H]raclopride to human dopamine $D_2$ and $D_3$ receptors can be calculated by the saturation binding isotherm:

$$\text{Fractional occupancy} = \frac{[\text{Ligand}]}{[[\text{ligand}] + K_d]}$$

The total amount of receptor bound for [$^3$H]**WC-10** and [$^3$H]raclopride can be expressed by formula:

$$[^3\text{H}]\text{WC}-10\text{: } a_1D_2 + b_1D_3 = B_1$$

$$[^3\text{H}]\text{Raclopride: } a_2D_2 + b_2D_3 = B_2$$

Where $a_1$ and $b_1$ are the fractional occupancies of [$^3$H]**WC-10** to $D_2$ and $D_3$ receptors; $B_1$ is the total receptor density ($D_2/D_3$) directly measured from autoradiography studies of [$^3$H]**WC-10**; $a_2$, $b_2$, and $B_2$ are the same parameters for [$^3$H]raclopride; $D_2$, $D_3$ is the absolute density of $D_2$ and $D_3$ receptors. The absolute densities of $D_2$ and $D_3$ receptors can be calculated by solving the simultaneous equations:

$$D_2 = \frac{b_2B_1\text{-}b_1B_2}{a_1b_2\text{-}a_2b_1} \quad D_3 = \frac{a_1B_2\text{-}a_2B_1}{a_1b_2\text{-}a_2b_1}$$

**Statistical analysis.** The receptor-bound radioligand binding apparent densities were calculated using the specific activity of each radioligand expressed as fmol/mg tissue as previously described [18]. The experimenter was blinded to all conditions during the analysis. Comparison of receptor densities was analyzed by an unpaired Student's t test. Assessment of correlation between different receptors binding was calculated using Pearson product moment correlation coefficient.

## Results

### Quantitative autoradiography

The sensitivity limit of Beta Imager 2000Z Digital Beta Imaging System is 0.07 dpm/mm$^2$. A tritium standard [$^3$H]Microscale with a known amount of radioactivity (ranging from 0 to 36.3 nCi/mg) was counted with each section and used to create a standard curve; in each case the standard curve had a correlation coefficient (R) greater than 0.99. On the basis of the saturation binding analysis and the *in vitro* binding data of [$^3$H]**WC-10** and [$^3$H]raclopride to cloned human $D_2$ and $D_3$ receptors [19], $K_d$ value and fractions of $D_2$ and $D_3$ receptor occupancies with 3.54 nM [$^3$H]**WC-10** and 2.50 nM [$^3$H]raclopride binding in human brain can be readily determined. The values of $K_d$ and receptors occupancies fractions are summarized in Figure 1.

### Quantitative analysis of dopamine $D_1$, $D_2$, $D_3$ receptors, DAT and VMAT2 densities in aged human brain

The binding densities of dopamine $D_1$ receptor, DAT and VMAT2 were determined by quantitative autoradiography using 1.44 nM [$^3$H]SCH23390, 2.19 nM [$^3$H]WIN355428 and 4.53nM [$^3$H]DTBZ, respectively. The apparent receptor binding densities ($B_1$ and $B_2$) of $D_2$ plus $D_3$ receptors were measured by using 3.54 nM [$^3$H]**WC-10** and 2.50 nM [$^3$H]raclopride respectively, and the absolute $D_2$ and $D_3$ receptors densities were determined as described above. The nonspecific binding was determined by using different high affinity cold compounds (Figures 2B, 3B, 4B, 5B). The receptor density values are summarized in Table 2.

**Precommissural striatal regions.** Dopamine $D_1$, $D_2$ and $D_3$ receptors were found to be extensively distributed throughout the precommissural striatal regions. The dopamine $D_3$ receptor density was much lower than that of the $D_1$ and $D_2$ receptors (Table 2; Figure 2). The dopamine $D_3$ receptor density was significantly lower in the putamen ($p = 0.001$) and caudate ($p = 0.0001$) than that of the NAc (Figure 1E). No difference in the $D_3$ receptor density was found between the putamen and caudate. The dopamine $D_2$:$D_3$ receptor density ratio was significantly higher in the putamen ($p = 0.04$) and caudate ($p = 0.04$) compared to that of the NAc, but was not different between the caudate and putamen (Figure 1F). The VMAT2 density was found to be ~10-fold higher than that of DAT in this region. Densities of DAT and VMAT2 were similar among the three sections of the precommissural striatal regions; an exception was the putamen, which showed significant increase in VMAT2 density versus that of the NAc ($P = 0.01$) (Figure 1E).

**Globus pallidus.** The density of dopamine $D_1$ and $D_2$ receptors, and DAT and VMAT2 were dramatically lower in the GP, whereas the density of the dopamine $D_3$ receptor was just slightly lower when compared to those of the striatal regions (Table 2; Figure 3). The distribution of dopamine receptors was different between the GPe and GPi: the dopamine $D_1$, $D_2$, and $D_3$ receptor densities were similar in the GPe, while the dopamine $D_1$ receptor density was significantly higher ($p = 0.02$) and the $D_2$ receptor density was significantly lower ($p = 0.03$) in the GPi compared to that of GPe (Figure 3E). Because of the lower density of dopamine $D_2$ receptors in the GPi, the dopamine $D_2$:$D_3$ receptor density ratio was significantly lower than that of GPe (Figure 3F). A lower level of VMAT2 density was distributed in both regions of the GP, whereas the density of the DAT was negligible compared to that in the striatal regions (Table 2; Figure 3E).

**Thalamus.** Dopamine $D_1$ receptor density was much lower and the $D_2$ receptor was negligible in the thalamus compared to those of the striatal regions (Table 2; Figure 4A, E). In contrast, the dopamine $D_3$ receptor density exceeded that observed in striatal regions, resulting in a low $D_2$:$D_3$ receptor density ratio in the thalamus ($0.11 \pm 0.05$) compared to that of the striatal regions (Figure 4F). A strong linear correlation ($R^2 > 0.78$) between the average density of dopamine $D_1$ and $D_3$ receptors was found in the thalamus (Figure 4G). A lower level of VMAT2 was found in the thalamus, whereas DAT density was nearly zero (Table 2; Figure 4A, E).

**Postcommissural striatal regions.** There were no significant differences in dopamine $D_2$ and $D_3$ receptor densities, and the $D_2$:$D_3$ receptor density ratio, between the pre- and postcommissural striatal regions. However, the dopamine $D_1$ receptor density was found to be significantly lower in the postcommissural putamen ($p = 0.01$) and caudate ($p = 0.01$) compared to their precommissural counterparts. The DAT density was found to be significantly decreased in the post- versus precommissural putamen ($p = 0.04$), while the VMAT level did not change.

**Substantia nigra.** Dopamine $D_1$ and $D_2$ receptor densities were much lower in the SN compared to those of the striatal regions. In contrast, the dopamine $D_3$ receptor density in the SN was the highest among the extrastriatal regions, and is only slightly lower than that of NAc (Table 2; Figure 5D). Consequently, the dopamine $D_2$:$D_3$ receptor density ratio in the SN was very low (Figure 5E). There was a moderate density of VMAT2 in the SN, while DAT density was negligible in this region (Figure 5D).

**Red nucleus.** Receptor densities in red nucleus (RN) were extremely low except for the dopamine $D_3$ receptor, which showed a relatively high density in this area (Table 2; Figure 5D). The dopamine $D_2$:$D_3$ receptor density ratio in the RN was similar as that of SN (Figure 5E).

### Comparison of dopamine $D_1$, $D_2$, and $D_3$ receptors, and DAT and VMAT2 densities in the striatal regions between aged rhesus monkey and aged human brain

To investigate the species differences of dopamine receptors and presynaptic markers, we compared the density of dopamine $D_1$, $D_2$, and $D_3$ receptors and DAT and VMAT2 in the striatal regions of an aged rhesus monkey (25 years old ) to those of aged human brain (average age: 91 years old). The densities of dopamine $D_1$ and $D_2$ receptors and DAT were found to be lower in aged human brain compared to those of rhesus monkey, whereas the dopamine $D_3$ receptor and VMAT2 densities were similar between these two species (Table 3; Figure 6).

### Different regulation of VMAT2 and DAT in the striatal regions and substantia nigra of aged human brain

In all brain regions measured, the VMAT2 density was found to be significantly higher than that of the DAT (Table 2). The VMAT2:DAT density ratio was regionally-dependent: the VMAT2 density was 30-fold higher than that of the DAT in the SN but only 10-fold higher in the precommissural striatal regions (Figure 7D). The average VMAT2 density strongly linearly correlated with DAT densities in the precommissural putamen ($r^2 = 0.68$) and caudate ($r^2 = 0.73$), but not in the SN ($r^2 < 0.01$) (Figure 7A). The VMAT2 density in the SN significantly correlated with those in the precommissural putamen ($r^2 = 0.60$) (Figure 7B) and caudate ($r^2 = 0.50$), but no such correlation was found for the DAT either in the precommissural putamen ($r^2 = 0.10$) or caudate ($r^2 = 0.11$) (Figure 7C).

## Discussion

Our group had previously reported the density of dopamine $D_2$ and $D_3$ receptors in rat and rhesus monkey brain using a novel

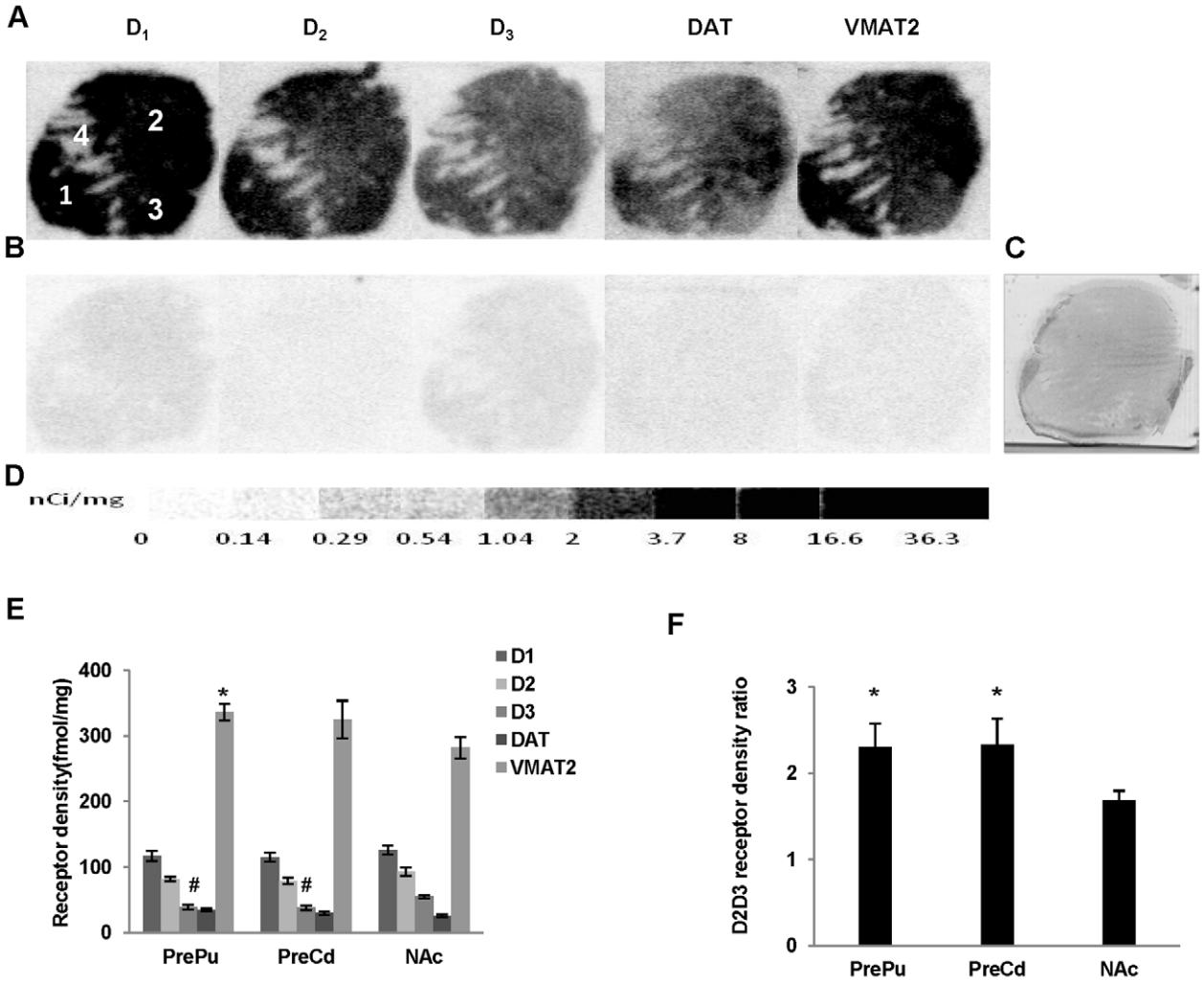


**Figure 2. Quantitative autoradiographic analysis of dopamine receptors, DAT and DTBZ densities in the precommissural striatal regions.** Autoradiograms show total binding of 1.44 nM [$^3$H]SCH23390, 2.50 nM[$^3$H]raclopride, 3.54 nM [$^3$H]**WC-10**, 2.19 nM [$^3$H]WIN35428, and 4.53 nM [$^3$H]DTBZ (A), and nonspecific binding in presence of 1 μM (+) butaclamol (for [$^3$H]SCH23390), 1 μM *S*(-)-eticlopride (for [$^3$H]raclopride and [$^3$H]**WC-10**), 1 μM nomifensine (for WIN35428) and 1 μM *S*(-)-tetrabenazine (for DTBZ) (B) in the precommissural striatal regions of human brain sections. The adjacent section shows cresyl violet staining to identify related anatomical structures (C). [$^3$H]Microscale standards (ranging from 0 to 36.3 nCi/mg) were also counted (D). Quantitative analysis of dopamine $D_1$, $D_2$, and $D_3$ receptors, and DAT and DTBZ densities (fmol/mg) and the dopamine $D_2$ : $D_3$ receptor density ratio in human striatal regions are shown in E and F respectively. The numbers 1 through 4 designate the following CNS anatomical regions: 1: Precommissural Putamen (PrePu); 2: Precommissural caudate (PreCd);3: Nucleus accumbens (NAc); 4: Internal capsule (IC). *$p<0.05$, #$p<0.01$ compared to NAc.
doi:10.1371/journal.pone.0049483.g002

autoradiography method involving the use of two different radioligands, the $D_3$-preferring ligand [$^3$H]WC-10 and the $D_2$/$D_3$ nonselective ligand [$^3$H]raclopride [18]. Here we report first measurements of $D_2$ and $D_3$ specific receptors in aged human postmortem brain. We also included measurements of the density of dopamine $D_1$ receptors, DAT and VMAT2 using well-established tritiated ligands and quantitative autoradiography. Some noteworthy findings include: 1) $D_3$ receptors were widely distributed throughout the striatal and extrastriatal regions in the aged human brain; 2) in the striatal regions, $D_3$ receptors were more enriched in the NAc than in the caudate and putamen; 3) in the extrastriatal regions, dopamine $D_3$ receptor density exceeded $D_2$ receptors; 3) DAT density in aged human brain was more than 10-fold lower than that of VMAT2 in the striatal regions, and was negligible in the SN, whereas VMAT2 density was relatively high; 4) receptor densities of dopamine $D_1$, $D_2$ and DAT was lower in human versus monkey brain, but $D_3$ and VMAT2 densities appeared to be similar.

Quantitative autoradiography to measure dopamine $D_3$ receptor density have previously been conducted using radiolabeled agonists such as [$^3$H]7-OH-DPAT, [$^{125}$I]PIPAT, and [$^3$H]PD 128907. Since these ligands bind to both the $D_3$ receptor and the dopamine "high affinity binding site" of the $D_2$ receptor [26], the $D_2$ receptor must first be "decoupled" to form the dopamine low affinity agonist binding state in order to measure $D_3$ receptors with these radioligands [13–15,27,28]. Other studies have used radiolabeled $D_2$/$D_3$ antagonists in the presence of a $D_2$-preferring antagonist to determine the density of $D_2$ and $D_3$ receptors in autoradiography studies [12,16,17]. However, it is difficult to quantify $D_2$ and $D_3$ receptor density using this approach given the relatively low $D_2$/$D_3$ selectivity of the $D_2$-preferring blocking agent. Recently our lab has developed a new radiolabeled $D_3$

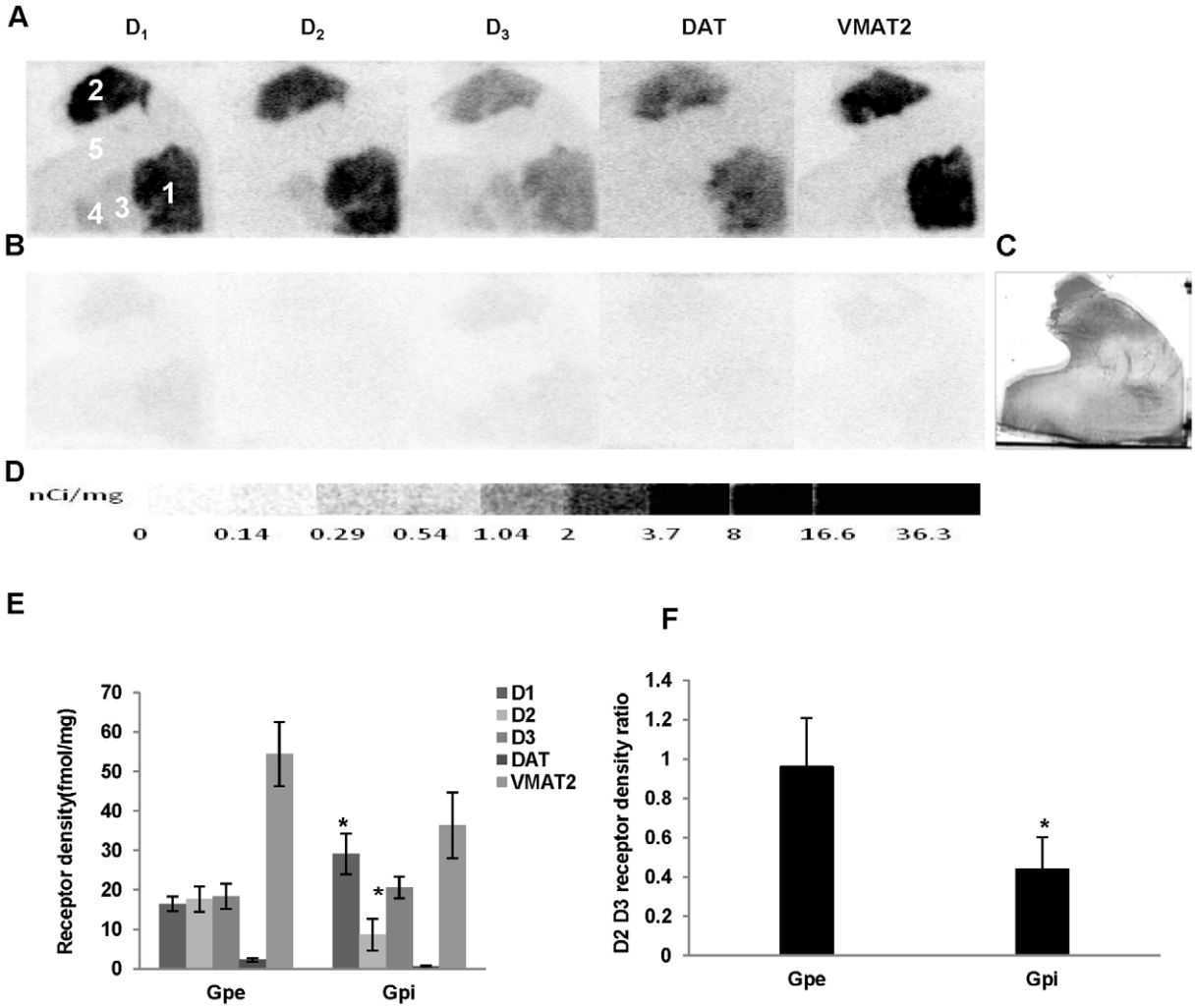


**Figure 3. Quantitative autoradiographic analysis of dopamine $D_3$ receptors, DAT and DTBZ densities in the globus pallidus.** Autoradiograms show total binding of 1.44 nM [$^3$H]SCH23390, 2.50 nM [$^3$H]raclopride, 3.54 nM [$^3$H]**WC-10**, 2.19 nM [$^3$H]WIN35428, 4.53 nM [$^3$H]DTBZ (A), and nonspecific binding in presence of 1 μM (+) butaclamol (for [$^3$H]SCH23390), 1 μM *S*(-)-eticlopride (for [$^3$H]raclopride and [$^3$H]**WC-10**), 1 μM nomifensine (for [$^3$H]WIN35428) and 1 μM *S*(-)-tetrabenazine (for [$^3$H]DTBZ) (B) in the globus pallidus of aged human brain sections. The adjacent section shows cresyl violet staining to identify related anatomical structures (C). [$^3$H]Microscale standards (ranging from 0 to 36.3 nCi/mg) were also counted (D). Quantitative analysis of dopamine $D_1$, $D_2$, and $D_3$ receptors, DAT and DTBZ densities (fmol/mg) and the dopamine $D_2$ : $D_3$ receptor density ratio in human globus pallidus are shown in E and F, respectively. The numbers 1 through 5 designate the following CNS anatomical regions: 1: Putamen; 2: Caudate; 3: Globus pallidus external part (GPe); 4: Globus pallidus internal part (GPi); 5: Internal capsule (IC). *$p<0.05$ compared to GPe.

doi:10.1371/journal.pone.0049483.g003

receptor antagonist/partial agonist [$^3$H]WC-10, which has high binding affinity and selectivity to $D_3$ versus $D_2$ receptors [19,20]. By combining autoradiography studies with [$^3$H]WC-10 with the $D_2/D_3$ nonselective ligand [$^3$H]raclopride, the density of dopamine $D_2$ and $D_3$ receptors can be easily determined using the mathematical model [18].

The current finding of the dopamine $D_3$ receptor distribution pattern in the striatal regions is in agreement with some previous reports [13,14,18], but not consistent with other reports demonstrating a restricted distribution in the limbic areas of the striatum [17,29,30]. However, in situ hybridization studies have shown that dopamine $D_3$ receptor mRNA is found in the caudate, putamen and nucleus accumbens in human and monkey brain [13,31,32], which provides additional support for the current observations. The distribution of dopamine $D_3$ receptors in the putamen and caudate, with a higher density in the NAc, suggests that the dopamine $D_3$ receptor may also be involved in the regulation of locomotor function in addition to their well-recognized role in the limbic system.

The measurement of dopamine $D_3$ receptors in the GPi is consistent with previous publications [17]. Interestingly, the dopamine $D_1$ receptor density was found to be significantly higher and the $D_2$ receptor density significantly lower in the GPi versus GPe, which is in agreement with the recent finding showing the similar distribution of dopamine $D_1$ and $D_2$ receptors in the globus pallidus by using bacterial artificial chromosome (BAC) transgenic mice in which expression of enhanced green fluorescent protein (eGFP), is driven by the promoter region of either the $D_1$ or the $D_2$ [33]. The different distribution pattern of the dopamine $D_1$ and $D_2$ receptors in the GPe and GPi found in this study has provided the additional proof that the $D_1$ receptormediated direct pathway

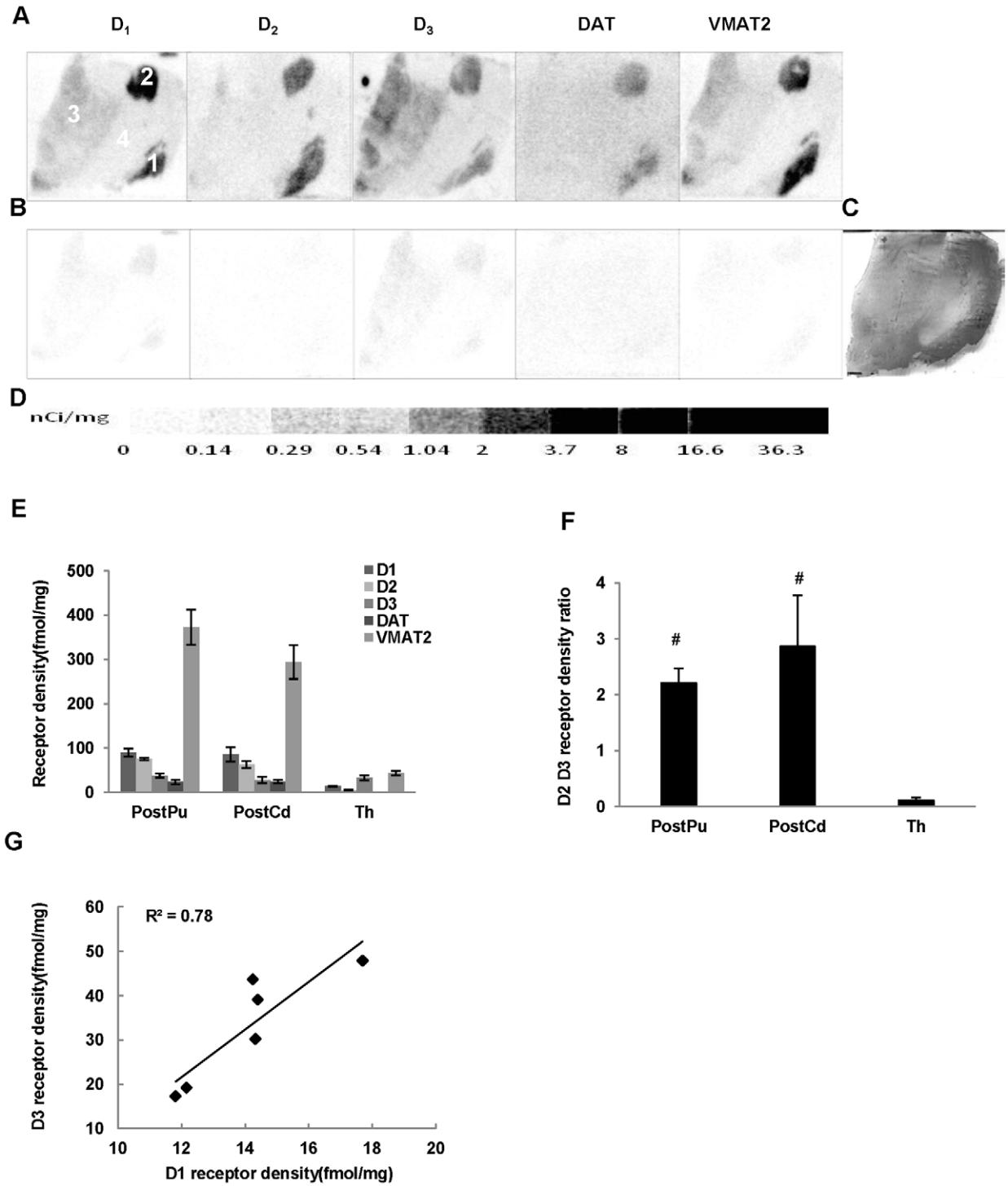


**Figure 4. Quantitative autoradiographic analysis of dopamine receptors, DAT and DTBZ densities in the thalamus.** Autoradiograms show total binding of 1.44 nM [$^3$H]SCH23390, 2.50 nM [$^3$H]raclopride, 3.54 nM [$^3$H]**WC-10**, 2.19 nM [$^3$H]WIN35428, 4.53 nM [$^3$H]DTBZ (A), and nonspecific binding in presence of 1 μM (+) butaclamol (for [$^3$H]SCH23390), 1 μM *S*(-)-eticlopride (for [$^3$H]raclopride and [$^3$H]**WC-10**), 1 μM nomifensine (for WIN35428) and 1 μM *S*(-)-tetrabenazine (for DTBZ) (B) in the thalamus of human brain sections. The adjacent section shows cresyl violet staining to identify related anatomical structures (C). [$^3$H]Microscale standards (ranging from 0 to 36.3 nCi/mg) were also counted (D). Quantitative analysis of dopamine $D_1$, $D_2$, and $D_3$ receptors, DAT and DTBZ densities (fmol/mg) and the dopamine $D_2$ : $D_3$ receptor density ratio in human brain are shown in E and F, respectively. Linear correlation analysis of the average dopamine $D_1$ and $D_3$ receptor densities in human thalamus is shown in (G). The numbers 1 through 4 designate the following CNS anatomical regions: 1: Postcommissural putamen (PostPu); 2: Postcommissural caudate (PosCd); 3: Thalamus; 4: Internal capsule (IC). #$p<0.01$ compared to thalamus.
doi:10.1371/journal.pone.0049483.g004

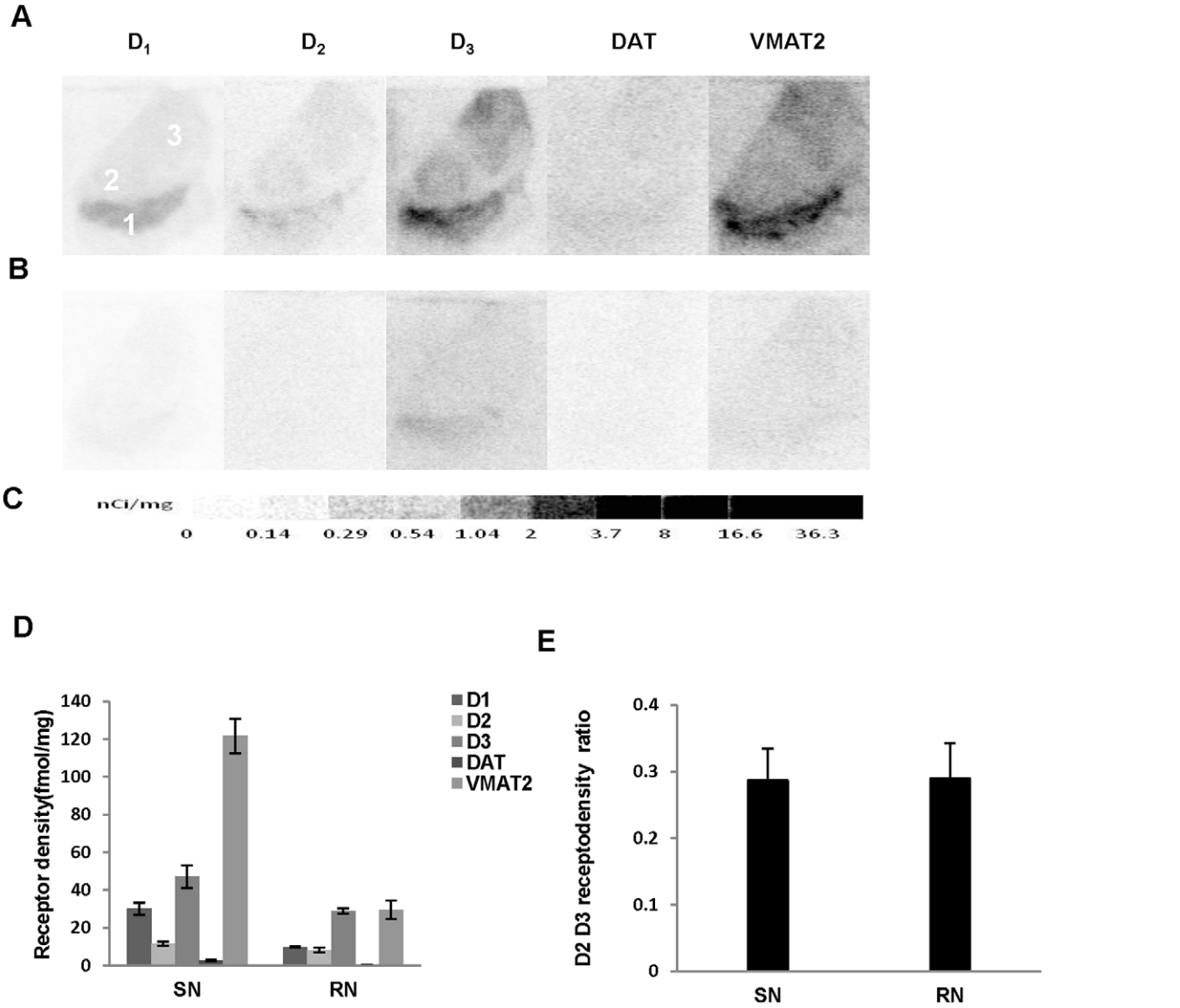


**Figure 5. Quantitative autoradiographic analysis of dopamine receptors, and DAT and DTBZ densities in the substantia nigra.** Autoradiograms show total binding of 1.44 nM [$^3$H]SCH23390, 2.50 nM[$^3$H]raclopride, 3.54 nM [$^3$H]**WC-10**, 2.19 nM [$^3$H]WIN35428, 4.53 nM [$^3$H]DTBZ (A), and nonspecific binding in presence of 1 uM (+) butaclamol (for [$^3$H]SCH23390), 1 μM *S*(-)-eticlopride (for [$^3$H]raclopride and [$^3$H]**WC-10**), 1 μM nomifensine (for WIN35428) and 1 μM *S*(-)-tetrabenazine (for DTBZ) (B) in the substantia nigra (SN) of aged human brain sections. [$^3$H]Microscale standards (ranging from 0 to 36.3 nCi/mg) were also counted (C). Quantitative analysis of dopamine $D_1$, $D_2$ and $D_3$ receptors, and DAT and DTBZ densities (fmol/mg) and the dopamine $D_2$ : $D_3$ receptor density ratio in human SN and red nucleus are shown in D and E respectively. The numbers 1 through 3 designate the following CNS anatomical regions: 1: Substantia nigra (SN); 2: Red nucleus (RN); 3: Thalamus.
doi:10.1371/journal.pone.0049483.g005

going from striatum to GPi and the $D_2$ receptor mediated indirect pathway going from striatal to GPe.

The thalamus is another interesting target for brain dopamine [34]. Previous receptor autoradiography studies with the radioligand [$^{125}$I]epidepride found a modest density of dopamine $D_2$-like receptors in the thalamus [12,35]. On the other hand, dopamine $D_3$ receptor density was found to be very low in human thalamus when [$^3$H]7-OH-DPAT was used as the radioligand [13]. In PET imaging studies, radiotracers such as [$^{18}$F]fallypride which has a high affinity for both $D_2$ and $D_3$ receptors, and [$^{11}$C]PHNO which is a $D_3$ preferring ligand, , display a high uptake in the thalamus of human and monkey brain [9,36–40]. This is in contrast to [$^{18}$F]NMB and [$^{11}$C]raclopride, both tracers have lower uptakes in the thalamus versus the striatum and putamen [41,42]; NMB and raclopride have higher affinities for $D_2$ versus $D_3$ receptors, which could explain their relatively low uptake in the thalamus. In the present study, dopamine $D_3$ receptors were found to be abundant while the $D_2$ receptor was nearly negligible in the thalamus of aged human brain. Consequently, the dopamine $D_2$:$D_3$ receptor density ratio was very low in this area. Although the current autoradiography study was conducted in aged subjects with no sign of neurological disease, it is not likely that the aging process would result in a complete loss of dopamine $D_2$ receptors in lieu of $D_3$ receptors. Therefore, our data indicate that the thalamus can be used as a good region to study dopamine $D_3$ receptor function in PET imaging studies using radiotracers such as [$^{18}$F]fallypride,

**Table 2.** Dopamine $D_1$, $D_2$, $D_3$ receptors, dopamine transporter (DAT) and vesicular monoamine transporter type-2 (VMAT2) densities and $D_2$ : $D_3$ receptor density ratio in aged human brain.

| Region | Region abbreviation | DAT | VMAT2 | $D_1$ | $D_2$ | $D_3$ | $D_2D_3$ ratio | n |
|---|---|---|---|---|---|---|---|---|
| Precommissural putamen | PrePu | 35±3 | 336±13 | 117±7 | 82±3 | 39±3 | 2.30±0.28 | 10 |
| Precommissural caudate | PreCd | 30±4 | 325±29 | 115±7 | 79±5 | 38±4 | 2.29±0.27 | 10 |
| Nucleus accumbens | NAc | 26±5 | 282±16 | 126±7 | 93±6 | 55±2 | 1.69±0.11 | 8 |
| Postcommissural putamen | PosPu | 24±5 | 373±39 | 90±9 | 76±3 | 38±5 | 2.21±0.27 | 7 |
| Postcommissural caudate | PosCd | 24±3 | 294±38 | 86±16 | 63±7 | 28±7 | 2.87±0.91 | 4 |
| Globus pallidus external part | GPe | 2±0.4 | 54±8 | 16±2 | 18±3 | 18±3 | 0.96±0.25 | 6 |
| Globus pallidus internal part | GPi | 0.6±0.3 | 36±8 | 29±5 | 9±4 | 21±3 | 0.44±0.16 | 6 |
| Thalamus | Th | 0.8±0.4 | 44±5 | 14±1 | 4±2 | 33±5 | 0.11±0.05 | 6 |
| Substantia nigra | SN | 4±0.4 | 122±9 | 30±3 | 13±1 | 47±6 | 0.30±0.05 | 8 |
| Red nucleus | RN | 4±0.3 | 30±5 | 10±0.9 | 8±1 | 29±1 | 0.29±0.05 | 6 |

Receptor densities (fmol/mg) presented as mean value ±SEM.
doi:10.1371/journal.pone.0049483.t002

[$^{11}$C]raclopride, and [$^{11}$C]PHNO. It should be noted that differences in the $D_2/D_3$ binding potential of these PET radiotracers in the thalamus have been reported in a variety of neurological and neuropsychiatric disorders, including schizophrenia [43–46], substance abuse [47,48] and dystonia [49,50] relative to age-matched controls. The finding of the high $D_3$ receptor density and low $D_2$:$D_3$ ratio in the human thalamus indicates that the changes of $D_2/D_3$ thalamic binding potential in these patients measured by PET may be attributed to changes in dopamine $D_3$ receptor function, and that dopamine $D_3$ receptors may play a key role in the pathophysiology of these disorders.

The dopamine $D_3$ receptor was also found to be abundantly distributed in the SN and RN, whereas the density of $D_2$ receptors was lower. Dopamine $D_2$-like receptors were observed in the RN and SN with high and moderate density in a human PET imaging study using [$^{11}$C]FLB 457 [51]. More recent studies using the dopamine $D_3$-preferring agonist [$^{11}$C]PHNO [38], reported a high density of dopamine $D_3$ receptors and negligible $D_2$ receptors in the SN [40,52–55], which is consistent with our autoradiography findings. The dopamine $D_1$ receptor was also found to be present in the SN with a density intermediate to $D_3$ and $D_2$ receptors, which agrees with previous reports [56–58]. The abundance of dopamine $D_3$ receptors and lower $D_2$:$D_3$ receptor

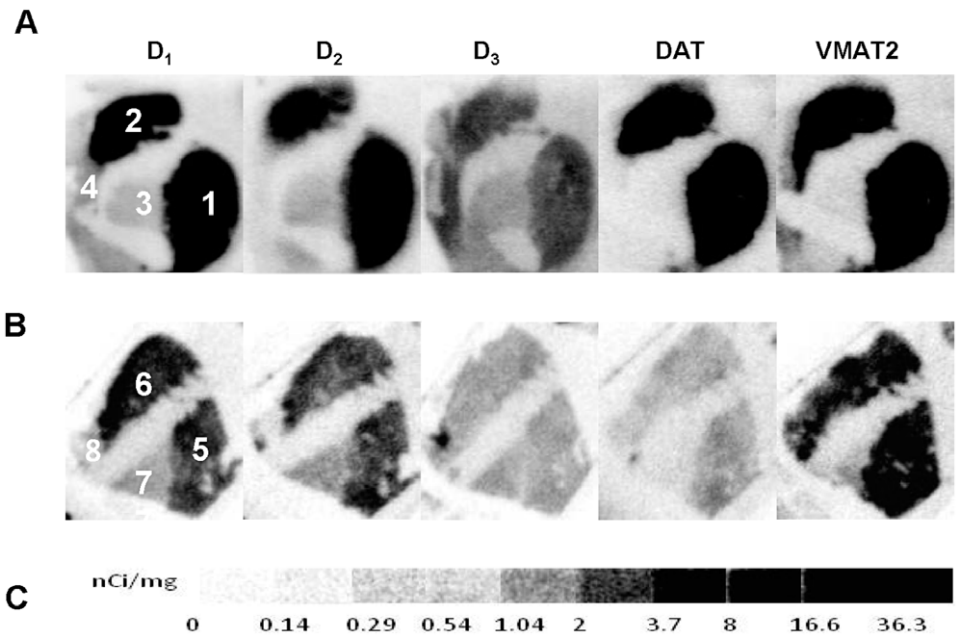


**Figure 6. Comparison of dopamine $D_1$, $D_2$, and $D_3$ receptors, and DAT and DTBZ densities in the striatal regions between an aged rhesus monkey (25 years old) and aged human brain samples.** Autoradiograms show neuroanatomical localization of [$^3$H]SCH23390 for $D_1$, [$^3$H]raclopride for $D_2$, [$^3$H]**WC-10** for $D_3$ receptors, [$^3$H]WIN35428 for DAT and [$^3$H]DTBZ for VMAT2 in the striatal regions of rhesus monkey (A) and aged human brain (B). [$^3$H]Microscale stnadards (ranging from 0 to 36.3 nCi/mg) (C). The numbers 1 through 8 in panels (A) (B) designate the following CNS anatomical regions: 1: Monkey putamen; 2: Monkey caudate; 3: Monkey globus pallidus; 4: Monkey thalamus; 5: Human putamen; 6: Human caudate; 7: Human globus pallidus; 8: Human thalamus.
doi:10.1371/journal.pone.0049483.g006

**Table 3.** Comparison of dopamine $D_1$, $D_2$, $D_3$ receptors, DAT and VMAT2 densities (fmol/mg) in the striatal regions of adult rhesus monkey and aged human brain.

| | $D_1$ | | $D_2$ | | $D_3$ | | DAT | | VMAT2 | |
|---|---|---|---|---|---|---|---|---|---|---|
| | Pu | Cd | Pu | Cd | Pu | Cd | Pu | Cd | Pu | Cd |
| Rhesus monkey | 256±19 | 228±9 | 178±9 | 205±6 | 36±9 | 46±4 | 185±12 | 177±17 | 341±20 | 351±10 |
| Human | 117±23 | 119±16 | 82±11 | 77±15 | 39±11 | 36±11 | 35±10 | 30±11 | 336±40 | 325±86 |

Data were obtained from 10 aged healthy human and a 25 years old rhesus monkey brain and presented as mean value ± stdev. Pu: Putamen; Cd: Caudate.
doi:10.1371/journal.pone.0049483.t003

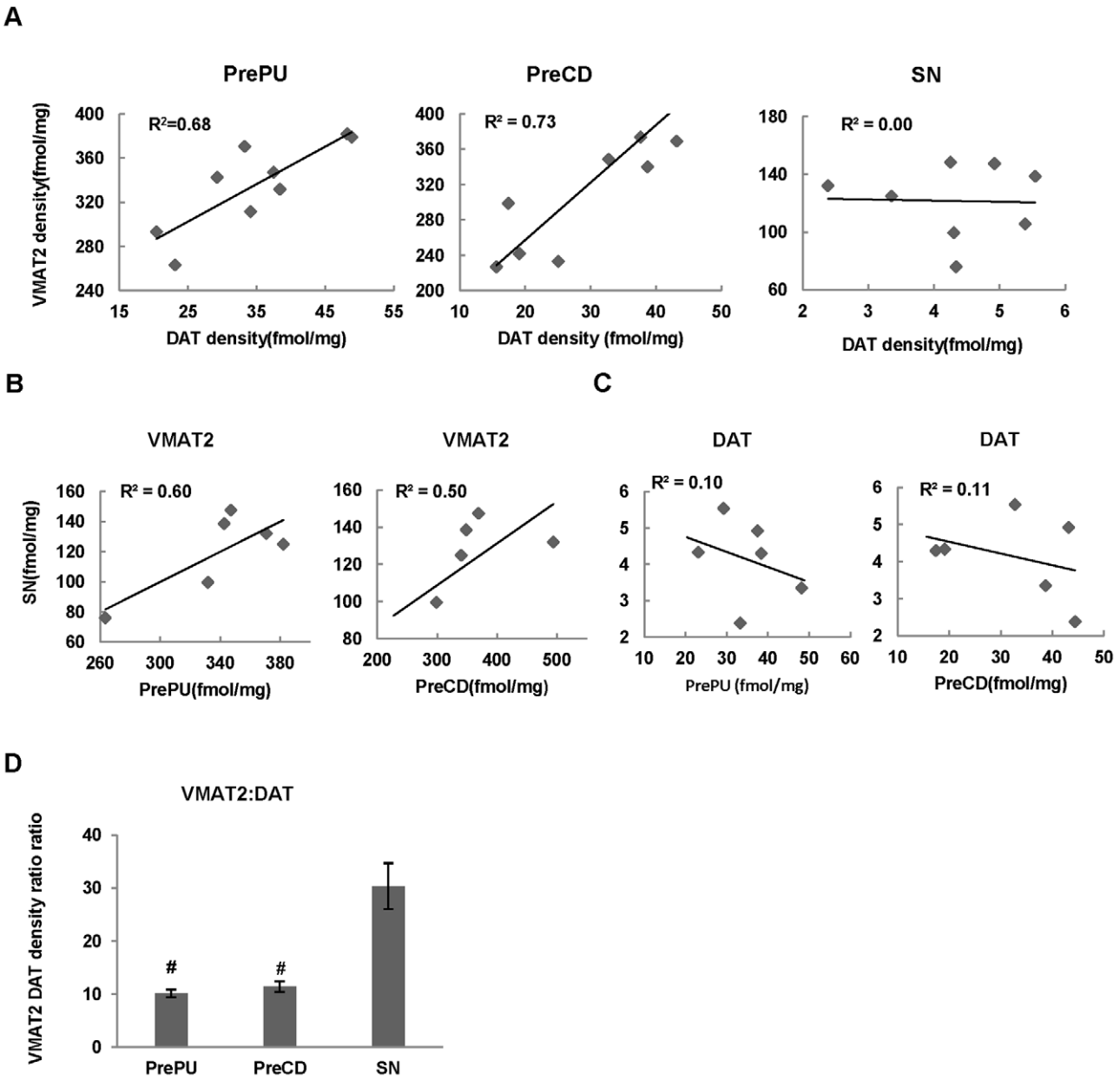


**Figure 7. Correlation of DAT with VMAT2 in the striatal regions and substantia nigra.** The correlation between the VMAT2 and DAT densities in the precommissural putamen (PrePu), caudate (PreCd) and substantia nigra (SN) (A). Correlation of the VMAT densities between the substantia nigra (SN) and PrePu or PreCd (B). Correlation of the DAT densities between the SN and PrePu or PreCd (C). The average VMAT DAT density ratio in the PrePu, PreCd and SN (D). #$p<0.01$ compared to SN.
doi:10.1371/journal.pone.0049483.g007

density ratio in human SN represents a second region to study dopamine $D_3$ versus $D_2$ effects using currently available PET ligands. The functional significance of the abundant existence of $D_3$ versus $D_2$ receptors in human SN is not clear. One possible explanation is that dopamine $D_3$ receptors may be involved in the negative feedback regulation of tonic dopamine release.

A number of biochemical and behavioral studies have suggested that $D_1$ and $D_3$ receptors may functionally interact [59,60]. For example, $D_1$ and $D_3$ mRNAs are co-localized in a large number of neurons in the striatum [61] and the NAc [62–64], and co-activation of $D_1$ and $D_3$ receptors in the shell of the NAc synergistically increases substance P expression [63,64]. $D_1$ and $D_3$ interactions are thought to mediate the rewarding properties of low doses of cocaine [36], and L-DOPA administration to rats receiving a unilateral injection of the neurotoxin 6-OH-dopamine results in an overexpression of $D_3$ receptors in nigrostriatal neurons that constitutively express $D_1$ receptors [59,65,66]. Dopamine $D_1$ and $D_3$ receptors were co-expressed in the renal proximal tubule [67] and in transfected HEK-293 cells [68]. Heterodimerization of these two receptors has been observed by co-immunoprecipitation from striatal protein preparations [59] or by bioluminescence resonance energy transfer technique in transfected mammalian cells [59,68]. It is of interest to note that a linear correlation of dopamine $D_1$ and $D_3$ receptor densities was found in the thalamus, which is consistent with either an anatomical or functional coupling of $D_1$ and $D_3$ dopamine receptor subtypes. $D_1$ receptors are not thought to interact with $D_3$ receptors functioning as autoreceptors [60]; and we found no strong correlation of $D_1$ and $D_3$ receptor density in the caudate, putamen and SN (data not shown), where $D_3$ receptors may function as autoreceptors. The availability of [$^3$H]**WC-10**, a $D_3$-preferring radioligand, will provide a valuable tool for studying the functional interactions between dopamine $D_1$ and $D_3$ receptors in the CNS.

The DAT and VMAT2 distribution pattern found in this study is consistent with the previous reports [69–72].The higher density level of both DAT and VMAT2 was found in the putamen and caudate compared to that of nucleus accumbens, which is in line with the recent finding using the same radioligands [73]. Surprisingly the DAT density was 10 fold lower than that of VMAT2 in aged human striatum which is different from previous reports. Furthermore the DAT density was lower while the VMAT2 density was not significantly different in the aged human compared to that of monkey brain. This may reflect the different aging related change patterns of these two dopamine presynaptic markers. In fact aging related decline of DAT but not VMAT2 density in the human brain has been reported [74–76]. In the striatal regions, the DAT density was significantly correlated with that of the VMAT2, indicating the anatomical and functional coupling of these two presynaptic dopamine markers.

The monkey brain had a higher density of $D_1$ and $D_2$ receptors relative to the human brain, but a similar density of $D_3$ receptors. Dopamine $D_1$ [58,77–79] and $D_2$ [46,80–82] receptor densities decline with aging in human brain, but no reports have been published measuring the density of $D_3$ receptors as a function of age.

The main limitation of this study is absence of data from younger subjects. The results of this study may only reflect the densities and distribution of the dopamine receptors and transporters in advanced aged human brain, and may not reflect age-related changes of presynaptic and postsynaptic dopamine markers. Therefore, caution should be given when comparing these data with that of PET imaging studies of the dopaminergic in younger subjects.

## Conclusions

This study provides quantitative measurements of the density of presynaptic (VMAT2 and DAT) and postsynaptic dopaminergic markers (dopamine $D_1$, $D_2$, and $D_3$ receptors) in the aged human brain. The correlation between the density of $D_1$ and $D_3$ receptors in the thalamus, and the DAT and VMAT2 in the striatal regions, suggests a functional interaction between these markers. The high density of $D_3$ receptors in the thalamus and SN and low density of $D_2$ receptors in these brain regions could provide valuable information for PET imaging $D_3$ and $D_2$ receptor function using [$^{18}$F]fallypride, [$^{11}$C]raclopride, [$^{18}$F]NMB, and [$^{11}$C]PHNO. The differential density of $D_2$ and $D_3$ receptors in these brain regions can also be used in determining the *in vivo* selectivity on newer PET radiotracers which are being developed to discriminate between $D_3$ and $D_2$ receptors and vice versa.

## Acknowledgments

The authors thank Deborah Carter and Toral Patel of the Knight Alzheimer's Disease Research Center Neuropathology Core at Washington University School of Medicine, for expert technical assistance.

## Author Contributions

Conceived and designed the experiments: JX RHM. Performed the experiments: JS. Analyzed the data: JS JX JSP. Contributed reagents/materials/analysis tools: NJC. Wrote the paper: JS RHM.

## References

1. Abi-Dargham A, Rodenhiser J, Printz D, Zea-Ponce Y, Gil R, et al. (2000) Increased baseline occupancy of D2 receptors by dopamine in schizophrenia. Proc Natl Acad Sci USA 97: 8104–8109.
2. Micheli F, Bonanomi G, Braggio S, Capelli AM, Celestini P, et al. (2008) New fused benzazepine as selective D3 receptor antagonists. Synthesis and biological evaluation. Part one: [h]-fused tricyclic systems. Bioorg Med Chem Lett 18: 901–907.
3. Sokoloff P, Diaz J, Le Foll B, Guillin O, Leriche L, et al. (2006) The dopamine D3 receptor: a therapeutic target for the treatment of neuropsychiatric disorders. CNS Neurol Disord Drug Targets 5: 25–43.
4. Volkow ND, Fowler JS, Wolf AP, Schlyer D, Shiue CY, et al. (1990) Effects of chronic cocaine abuse on postsynaptic dopamine receptors. Am J Psychiatry 147: 719–724.
5. Luedtke RR, Mach RH (2003) Progress in developing D3 dopamine receptor ligands as potential therapeutic agents for neurological and neuropsychiatric disorders. Curr Pharm Des 9: 643–671.
6. Neve KA, Seamans JK, Trantham-Davidson H (2004) Dopamine receptor signaling. J Recept Signal Transduct Res 24: 165–205.
7. Eiden LE, Schafer MK, Weihe E, Schutz B (2004) The vesicular amine transporter family (SLC18): amine/proton antiporters required for vesicular accumulation and regulated exocytotic secretion of monoamines and acetylcholine. Pflugers Arch 447: 636–640.
8. Ehrin E, Farde L, de Paulis T, Eriksson L, Greitz T, et al. (1985) Preparation of 11C-labelled Raclopride, a new potent dopamine receptor antagonist: preliminary PET studies of cerebral dopamine receptors in the monkey. Int J Appl Radiat Isot 36: 269–273.
9. Mukherjee J, Yang ZY, Brown T, Lew R, Wernick M, et al. (1999) Preliminary assessment of extrastriatal dopamine D-2 receptor binding in the rodent and nonhuman primate brains using the high affinity radioligand, 18F-fallypride. Nucl Med Biol 26: 519–527.
10. Willeit M, Ginovart N, Kapur S, Houle S, Hussey D, et al. (2006) High-affinity states of human brain dopamine D2/3 receptors imaged by the agonist [11C]-(+)-PHNO. Biol Psychiatry 59: 389–394.
11. Gurevich EV, Joyce JN (1999) Distribution of dopamine D3 receptor expressing neurons in the human forebrain: comparison with D2 receptor expressing neurons. Neuropsychopharmacology 20: 60–80.
12. Hall H, Farde L, Halldin C, Hurd YL, Pauli S, et al. (1996) Autoradiographic localization of extrastriatal D2-dopamine receptors in the human brain using [125I]epidepride. Synapse 23: 115–123.

13. Herroelen L, De Backer JP, Wilczak N, Flamez A, Vauquelin G, et al. (1994) Autoradiographic distribution of D3-type dopamine receptors in human brain using [3H]7-hydroxy-N,N-di-n-propyl-2-aminotetralin. Brain Res 648: 222–228.
14. Hurley MJ, Jolkkonen J, Stubbs CM, Jenner P, Marsden CD (1996) Dopamine D3 receptors in the basal ganglia of the common marmoset and following MPTP and L-DOPA treatment. Brain Res 709: 259–264.
15. Lahti RA, Roberts RC, Tamminga CA (1995) D2-family receptor distribution in human postmortem tissue: an autoradiographic study. Neuroreport 6: 2505–2512.
16. Murray AM, Ryoo H, Joyce JN (1992) Visualization of dopamine D3-like receptors in human brain with [125I]epidepride. Eur J Pharmacol 227: 443–445.
17. Murray AM, Ryoo HL, Gurevich E, Joyce JN (1994) Localization of dopamine D3 receptors to mesolimbic and D2 receptors to mesostriatal regions of human forebrain. Proc Natl Acad Sci U S A 91: 11271–11275.
18. Xu J, Hassanzadeh B, Chu W, Tu Z, Jones LA, et al. (2010) [3H]4-(dimethylamino)-N-(4-(4-(2-methoxyphenyl)piperazin-1-yl) butyl)benzamide: a selective radioligand for dopamine D(3) receptors. II. Quantitative analysis of dopamine D(3) and D(2) receptor density ratio in the caudate-putamen. Synapse 64: 449–459.
19. Xu J, Chu W, Tu Z, Jones LA, Luedtke RR, et al. (2009) [(3)H]4-(Dimethylamino)-N-[4-(4-(2-methoxyphenyl)piperazin- 1-yl)butyl]benzamide, a selective radioligand for dopamine D(3) receptors. I. In vitro characterization. Synapse 63: 717–728.
20. Chu W, Tu Z, McElveen E, Xu J, Taylor M, et al. (2005) Synthesis and in vitro binding of N-phenyl piperazine analogs as potential dopamine D3 receptor ligands. Bioorg Med Chem 13: 77–87.
21. Braak H, Alafuzoff I, Arzberger T, Kretzschmar H, Del Tredici K (2006) Staging of Alzheimer disease-associated neurofibrillary pathology using paraffin sections and immunocytochemistry. Acta Neuropathol 112: 389–404.
22. Braak H, Braak E, Bohl J, Reintjes R (1996) Age, neurofibrillary changes, A beta-amyloid and the onset of Alzheimer's disease. Neurosci Lett 210: 87–90.
23. Savasta M, Dubois A, Scatton B (1986) Autoradiographic localization of D1 dopamine receptors in the rat brain with [3H]SCH 23390. Brain Res 375: 291–301.
24. Lim MM, Xu J, Holtzman DM, Mach RH (2011) Sleep deprivation differentially affects dopamine receptor subtypes in mouse striatum. Neuroreport 22: 489–493.
25. Novick A, Yaroslavsky I, Tejani-Butt S (2008) Strain differences in the expression of dopamine D1 receptors in Wistar-Kyoto (WKY) and Wistar rats. Life Sci 83: 74–78.
26. Sibley DR, De Lean A, Creese I (1982) Anterior pituitary dopamine receptors. Demonstration of interconvertible high and low affinity states of the D-2 dopamine receptor. J Biol Chem 257: 6351–6361.
27. Bancroft GN, Morgan KA, Flietstra RJ, Levant B (1998) Binding of [3H]PD 128907, a putatively selective ligand for the D3 dopamine receptor, in rat brain: a receptor binding and quantitative autoradiographic study. Neuropsychopharmacology 18: 305–316.
28. Levesque D, Diaz J, Pilon C, Martres MP, Giros B, et al. (1992) Identification, characterization, and localization of the dopamine D3 receptor in rat brain using 7-[3H]hydroxy-N,N-di-n-propyl-2-aminotetralin. Proc Natl Acad Sci U S A 89: 8155–8159.
29. Landwehrmeyer B, Mengod G, Palacios JM (1993) Dopamine D3 receptor mRNA and binding sites in human brain. Brain Res Mol Brain Res 18: 187–192.
30. Morissette M, Goulet M, Grondin R, Blanchet P, Bedard PJ, et al. (1998) Associative and limbic regions of monkey striatum express high levels of dopamine D3 receptors: effects of MPTP and dopamine agonist replacement therapies. Eur J Neurosci 10: 2565–2573.
31. Meador-Woodruff JH, Damask SP, Wang J, Haroutunian V, Davis KL, et al. (1996) Dopamine receptor mRNA expression in human striatum and neocortex. Neuropsychopharmacology 15: 17–29.
32. Suzuki M, Hurd YL, Sokoloff P, Schwartz JC, Sedvall G (1998) D3 dopamine receptor mRNA is widely expressed in the human brain. Brain Res 779: 58–74.
33. Gerfen CR, Surmeier DJ (2011) Modulation of striatal projection systems by dopamine. Annu Rev Neurosci 34: 441–466.
34. Sanchez-Gonzalez JM, Rivera-Cisneros AE, Ramirez MJ, Tovar-Garcia Jde L, Portillo-Gallo J, et al. (2005) [Hydration status and aerobic capacity: effects on plasmatic volume during strenuous physical exercise]. Cir Cir 73: 287–295.
35. Rieck RW, Ansari MS, Whetsell WO Jr, Deutch AY, Kessler RM (2004) Distribution of dopamine D2-like receptors in the human thalamus: autoradiographic and PET studies. Neuropsychopharmacology 29: 362–372.
36. Karasinska JM, George SR, Cheng R, O'Dowd BF (2005) Deletion of dopamine D1 and D3 receptors differentially affects spontaneous behaviour and cocaine-induced locomotor activity, reward and CREB phosphorylation. Eur J Neurosci 22: 1741–1750.
37. Mukherjee J, Shi B, Christian BT, Chattopadhyay S, Narayanan TK (2004) 11C-Fallypride: radiosynthesis and preliminary evaluation of a novel dopamine D2/D3 receptor PET radiotracer in non-human primate brain. Bioorg Med Chem 12: 95–102.
38. Narendran R, Slifstein M, Guillin O, Hwang Y, Hwang DR, et al. (2006) Dopamine (D2/3) receptor agonist positron emission tomography radiotracer [11C]-(+)-PHNO is a D3 receptor preferring agonist in vivo. Synapse 60: 485–495.
39. Olsson H, Halldin C, Swahn CG, Farde L (1999) Quantification of [11C]FLB 457 binding to extrastriatal dopamine receptors in the human brain. J Cereb Blood Flow Metab 19: 1164–1173.
40. Tziortzi AC, Searle GE, Tzimopoulou S, Salinas C, Beaver JD, et al. (2011) Imaging dopamine receptors in humans with [11C]-(+)-PHNO: dissection of D3 signal and anatomy. Neuroimage 54: 264–277.
41. Eisenstein SA, Koller JM, Piccirillo M, Kim A, Antenor-Dorsey JA, et al. (2012) Characterization of extrastriatal D2 in vivo specific binding of [(18) F](N-methyl)benperidol using PET. Synapse 66: 770–780.
42. Te Beek ET, de Boer P, Moerland M, Schmidt ME, Hoetjes NJ, et al. (2012) In vivo quantification of striatal dopamine D2 receptor occupancy by JNJ-37822681 using [11C]raclopride and positron emission tomography. J Psychopharmacol.
43. Buchsbaum MS, Christian BT, Lehrer DS, Narayanan TK, Shi B, et al. (2006) D2/D3 dopamine receptor binding with [F-18]fallypride in thalamus and cortex of patients with schizophrenia. Schizophr Res 85: 232–244.
44. Kegeles LS, Slifstein M, Xu X, Urban N, Thompson JL, et al. (2010) Striatal and extrastriatal dopamine D2/D3 receptors in schizophrenia evaluated with [18F]fallypride positron emission tomography. Biol Psychiatry 68: 634–641.
45. Kessler RM, Woodward ND, Riccardi P, Li R, Ansari MS, et al. (2009) Dopamine D2 receptor levels in striatum, thalamus, substantia nigra, limbic regions, and cortex in schizophrenic subjects. Biol Psychiatry 65: 1024–1031.
46. Talvik M, Nordstrom AL, Olsson H, Halldin C, Farde L (2003) Decreased thalamic D2/D3 receptor binding in drug-naive patients with schizophrenia: a PET study with [11C]FLB 457. Int J Neuropsychopharmacol 6: 361–370.
47. Volkow ND, Fowler JS, Wang GJ (2002) Role of dopamine in drug reinforcement and addiction in humans: results from imaging studies. Behav Pharmacol 13: 355–366.
48. Volkow ND, Wang GJ, Fowler JS, Logan J, Angrist B, et al. (1997) Effects of methylphenidate on regional brain glucose metabolism in humans: relationship to dopamine D2 receptors. Am J Psychiatry 154: 50–55.
49. Carbon M, Niethammer M, Peng S, Raymond D, Dhawan V, et al. (2009) Abnormal striatal and thalamic dopamine neurotransmission: Genotype-related features of dystonia. Neurology 72: 2097–2103.
50. Perlmutter JS, Stambuk MK, Markham J, Black KJ, McGee-Minnich L, et al. (1997) Decreased [18F]spiperone binding in putamen in idiopathic focal dystonia. J Neurosci 17: 843–850.
51. Okubo Y, Olsson H, Ito H, Lofti M, Suhara T, et al. (1999) PET mapping of extrastriatal D2-like dopamine receptors in the human brain using an anatomic standardization technique and [11C]FLB 457. Neuroimage 10: 666–674.
52. Boileau I, Payer D, Houle S, Behzadi A, Rusjan PM, et al. (2012) Higher binding of the dopamine D3 receptor-preferring ligand [11C]-(+)-propyl-hexahydro-naphtho-oxazin in methamphetamine polydrug users: a positron emission tomography study. J Neurosci 32: 1353–1359.
53. Graff-Guerrero A, Redden L, Abi-Saab W, Katz DA, Houle S, et al. (2010) Blockade of [11C](+)-PHNO binding in human subjects by the dopamine D3 receptor antagonist ABT-925. Int J Neuropsychopharmacol 13: 273–287.
54. Rabiner EA, Slifstein M, Nobrega J, Plisson C, Huiban M, et al. (2009) In vivo quantification of regional dopamine-D3 receptor binding potential of (+)-PHNO: Studies in non-human primates and transgenic mice. Synapse 63: 782–793.
55. Searle G, Beaver JD, Comley RA, Bani M, Tziortzi A, et al. (2010) Imaging dopamine D3 receptors in the human brain with positron emission tomography, [11C]PHNO, and a selective D3 receptor antagonist. Biol Psychiatry 68: 392–399.
56. De Keyser J, Claeys A, De Backer JP, Ebinger G, Roels F, et al. (1988) Autoradiographic localization of D1 and D2 dopamine receptors in the human brain. Neurosci Lett 91: 142–147.
57. Mengod G, Villaro MT, Landwehrmeyer GB, Martinez-Mir MI, Niznik HB, et al. (1992) Visualization of dopamine D1, D2 and D3 receptor mRNAs in human and rat brain. Neurochem Int 20 Suppl: 33S–43S.
58. Palacios JM, Camps M, Cortes R, Probst A (1988) Mapping dopamine receptors in the human brain. J Neural Transm Suppl 27: 227–235.
59. Fiorentini C, Busi C, Gorruso E, Gotti C, Spano P, et al. (2008) Reciprocal regulation of dopamine D1 and D3 receptor function and trafficking by heterodimerization. Mol Pharmacol 74: 59–69.
60. Fiorentini C, Busi C, Spano P, Missale C (2010) Dimerization of dopamine D1 and D3 receptors in the regulation of striatal function. Curr Opin Pharmacol 10: 87–92.
61. Surmeier DJ, Song WJ, Yan Z (1996) Coordinated expression of dopamine receptors in neostriatal medium spiny neurons. J Neurosci 16: 6579–6591.
62. Le Moine C, Bloch B (1996) Expression of the D3 dopamine receptor in peptidergic neurons of the nucleus accumbens: comparison with the D1 and D2 dopamine receptors. Neuroscience 73: 131–143.
63. Ridray S, Griffon N, Mignon V, Souil E, Carboni S, et al. (1998) Coexpression of dopamine D1 and D3 receptors in islands of Calleja and shell of nucleus accumbens of the rat: opposite and synergistic functional interactions. Eur J Neurosci 10: 1676–1686.
64. Schwartz JC, Diaz J, Bordet R, Griffon N, Perachon S, et al. (1998) Functional implications of multiple dopamine receptor subtypes: the D1/D3 receptor coexistence. Brain Res Brain Res Rev 26: 236–242.

65. Bordet R, Ridray S, Schwartz JC, Sokoloff P (2000) Involvement of the direct striatonigral pathway in levodopa-induced sensitization in 6-hydroxydopamine-lesioned rats. Eur J Neurosci 12: 2117–2123.
66. Guillin O, Diaz J, Carroll P, Griffon N, Schwartz JC, et al. (2001) BDNF controls dopamine D3 receptor expression and triggers behavioural sensitization. Nature 411: 86–89.
67. Zeng C, Wang Z, Li H, Yu P, Zheng S, et al. (2006) D3 dopamine receptor directly interacts with D1 dopamine receptor in immortalized renal proximal tubule cells. Hypertension 47: 573–579.
68. Marcellino D, Ferre S, Casado V, Cortes A, Le Foll B, et al. (2008) Identification of dopamine D1–D3 receptor heteromers. Indications for a role of synergistic D1–D3 receptor interactions in the striatum. J Biol Chem 283: 26016–26025.
69. Canfield DR, Spealman RD, Kaufman MJ, Madras BK (1990) Autoradiographic localization of cocaine binding sites by [3H]CFT ([3H]WIN 35,428) in the monkey brain. Synapse 6: 189–195.
70. De La Garza R, 2nd, Meltzer PC, Madras BK (1999) Non-amine dopamine transporter probe [(3)H]tropoxene distributes to dopamine-rich regions of monkey brain. Synapse 34: 20–27.
71. Kaufman MJ, Spealman RD, Madras BK (1991) Distribution of cocaine recognition sites in monkey brain: I. In vitro autoradiography with [3H]CFT. Synapse 9: 177–187.
72. Scherman D, Raisman R, Ploska A, Agid Y (1988) [3H]dihydrotetrabenazine, a new in vitro monoaminergic probe for human brain. J Neurochem 50: 1131–1136.
73. Tian L, Karimi M, Loftin SK, Brown CA, Xia H, et al. (2012) No differential regulation of dopamine transporter (DAT) and vesicular monoamine transporter 2 (VMAT2) binding in a primate model of Parkinson disease. PLoS One 7: e31439.
74. Haycock JW, Becker L, Ang L, Furukawa Y, Hornykiewicz O, et al. (2003) Marked disparity between age-related changes in dopamine and other presynaptic dopaminergic markers in human striatum. J Neurochem 87: 574–585.
75. Troiano AR, Schulzer M, de la Fuente-Fernandez R, Mak E, McKenzie J, et al. (2010) Dopamine transporter PET in normal aging: dopamine transporter decline and its possible role in preservation of motor function. Synapse 64: 146–151.
76. Yue F, Zeng S, Wu D, Yi D, Alex Zhang Y, et al. (2012) Age-related decline in motor behavior and striatal dopamine transporter in cynomolgus monkeys. J Neural Transm.
77. Cortes R, Gueye B, Pazos A, Probst A, Palacios JM (1989) Dopamine receptors in human brain: autoradiographic distribution of D1 sites. Neuroscience 28: 263–273.
78. Jucaite A, Forssberg H, Karlsson P, Halldin C, Farde L (2010) Age-related reduction in dopamine D1 receptors in the human brain: from late childhood to adulthood, a positron emission tomography study. Neuroscience 167: 104–110.
79. Wang Y, Chan GL, Holden JE, Dobko T, Mak E, et al. (1998) Age-dependent decline of dopamine D1 receptors in human brain: a PET study. Synapse 30: 56–61.
80. Inoue M, Suhara T, Sudo Y, Okubo Y, Yasuno F, et al. (2001) Age-related reduction of extrastriatal dopamine D2 receptor measured by PET. Life Sci 69: 1079–1084.
81. Kaasinen V, Nagren K, Hietala J, Oikonen V, Vilkman H, et al. (2000) Extrastriatal dopamine D2 and D3 receptors in early and advanced Parkinson's disease. Neurology 54: 1482–1487.
82. Rinne JO, Hietala J, Ruotsalainen U, Sako E, Laihinen A, et al. (1993) Decrease in human striatal dopamine D2 receptor density with age: a PET study with [11C]raclopride. J Cereb Blood Flow Metab 13: 310–314.